

## Molten salt corrosion of Laser Cladding Stainless Steel

Jung-Min Kim<sup>a,b</sup>, Hyeon-Geun Lee<sup>b</sup>, Young-Bum Chun<sup>b</sup>, Chaewon Kim<sup>b</sup>

<sup>a</sup> University of Science and Technology, Daejeon 34113, KOREA

<sup>b</sup> Korea Atomic Energy Research Institute, 989-111 Daedeok-daero, Daejeon, 34057, KOREA

\*Corresponding author: hglee@kaeri.re.kr

\*Keywords : 316 stainless steel, Laser cladding, molten salt corrosion

### 1. Introduction

Molten-salt reactors (MSRs) operate at low pressure and have a reactor outlet temperature well above light water reactor technologies (typically 700°C or above). The critical issues that must be considered as the structural material for MSR include high-temperature strength, stability of microstructure, and properties for long-time thermal and environmental exposure, irradiation damage, fission product induced grain boundary embrittlement, and status of standardization and codification [1]. Upon this background, it may be possible to use Type 316 stainless steel [1]. The corrosion behavior of 316 stainless steel in a molten chloride salt was the selective diffusion of Cr element to the surface and the formation of Cr-compounds at the surface [2]. Also, for other Alloys, Cr depletion is reported as a major mechanism in molten salt corrosion [3, 4]. Particularly, intergranular corrosion, in which corrosion is selectively promoted at grain boundaries, was mainly observed. As a method of reducing grain boundary corrosion, a method of increasing the grain size is considered. Single-crystal stainless steel can be fabricated using laser cladding. The molten salt corrosion properties of single crystal 316 stainless steel fabricated by laser cladding were compared with commercial 316 stainless steel. The mass change was compared after corrosion in NaCl-MgCl<sub>2</sub> molten salt at 650°C for 620 h.

### 2. Experimental

316 stainless steels produced by laser cladding has been named as laser cladding, and the comparative commercial 316 stainless steel has been referred to wrought. The laser cladding specimens were made using the process conditions as follows; laser a power of 1800 W and scan speed 1000 mm/min. The specimens for microstructural observation were prepared for microstructural observation by grinding with SiC papers followed by vibratory polishing. Electron backscattered diffraction (EBSD) patterns were obtained using an EBSD detector from EDAX mounted on a JSM-7200F scanning electron microscope (SEM) operating at an accelerating voltage of 20 kV. For the molten salt corrosion test, the corrosion test was designed as shown in Figure 1. The inside of the

crucible was filled with Ar. Operations were performed in the glove box and oxygen and moisture were maintained below 10 ppm. NaCl-MgCl<sub>2</sub> eutectic salts (43% NaCl-57% MgCl<sub>2</sub>) were prepared by physical mixing. NaCl-MgCl<sub>2</sub> eutectic salts purified by heat treatment at 300 ° C for 48 hours and adding Mg to remove impurities such as moisture and oxygen. The molten salt corrosion samples were produced with a size of 10mm x 20mm x 1mm, and the surface was polished with SiC paper and finished with a 1um diamond suspension. The corrosion specimen was hung on a nickel wire and prevented from galvanic corrosion by alumina spacer. High temperature corrosion tests were performed at 650°C for up to 620 hours. Three specimens were taken at 100 hours, 500 hours, and 620 hours, respectively.

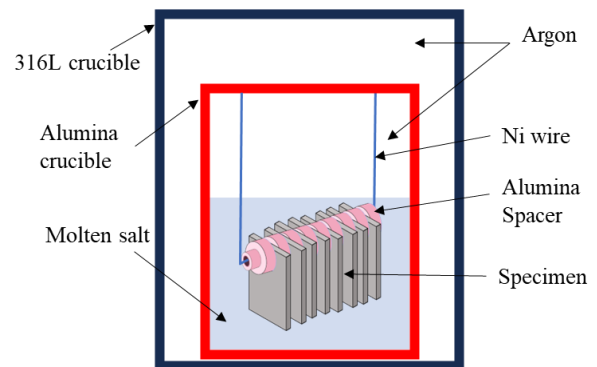


Fig. 1. Schematic illustration for Molten Salt Corrosion

### 3. Results

#### 3-1. Microstructure

Figure 2 shows microstructures of laser cladding and wrought by IPF map. The laser cladding specimen is almost single crystal and shows a very large grain size compared to the wrought specimen. The grain size measured by EBSD analysis is shown in Figure 3. The laser cladding specimen has a grain size about 16 times larger than that of the wrought specimen.

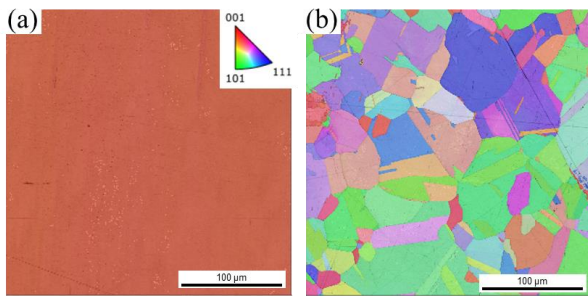


Fig. 2. IPF map of 316 specimens: (a) Wrought, (b) Laser Cladding.

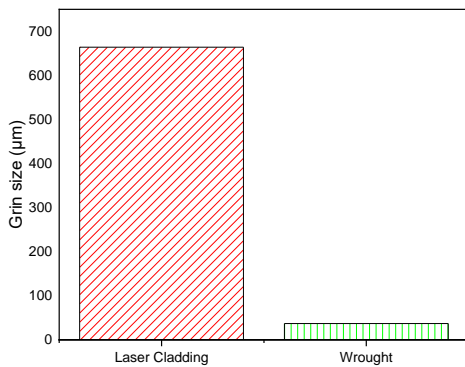


Fig. 3. Grain size of laser cladding specimen and wrought specimen.

### 3-2. Molten salt corrosion results

Figure 4 shows the corrosion rate of laser cladding and wrought specimens as function of exposure time. At exposure time of 100 hours, the corrosion rate of the laser cladding specimen and the wrought specimen were similar. For specimens exposed exceeding 500 hours, the corrosion rate of the laser cladding specimens was lower compared to that of the wrought specimens.

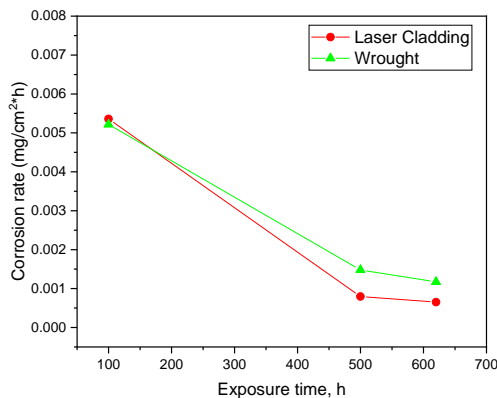


Fig. 4. Corrosion rate of laser cladding specimen and wrought specimen.

## 4. Conclusions

The effect of exposure time and laser cladding on the corrosion of 316 stainless steel in molten NaCl-MgCl<sub>2</sub> salts was studied through immersion corrosion for 100 h, 500h, and 620h.

The corrosion rate in NaCl-MgCl<sub>2</sub> salt at 650°C decreased with the increase in exposure time.

316 stainless steels fabricated with laser cladding showed better corrosion resistance than wrought 316 in molten salt.

This enhanced resistance is attributed to the reduced grain boundaries. The dominant mechanism of molten salt corrosion is believed to be grain boundary corrosion induced by chromium depletion. This will be proved through additional analysis such as EDS analysis and XRD analysis of the corrosion specimen.

## 5. Acknowledgments

This work was supported by the National Research Foundation of Korea (NRF) funded by Korea government (MSIT) (RS-2023-00229215).

## REFERENCES.

- [1] Wright, R. N., and T-L. Sham. Status of metallic structural materials for molten salt reactors. No. INL/EXT-18-45171-Rev000. Idaho National Lab.(INL), Idaho Falls, ID (United States); Argonne National Lab.(ANL), Argonne, IL (United States), 2018.
- [2] Ren, Sen, et al. Corrosion behavior of carburized 316 stainless steel in molten chloride salts. *Solar Energy* 223, 2021.
- [3] Bawane, Kaustubh, et al. Visualizing time-dependent microstructural and chemical evolution during molten salt corrosion of Ni-20Cr model alloy using correlative quasi in situ TEM and in situ synchrotron X-ray nano-tomography. *Corrosion Science* 195, 2022.
- [4] Danon, A. E., et al. Molten salt corrosion (FLiNaK) of a Ni-Mo-Cr alloy and its welds for application in energy-generation and energy-storage systems. *Corrosion Science* 164, 2020.